Appl. Phys. A 80, 557–563 (2005)
DOI: 10.1007/s00339-004-2967-5

Applied Physics A
Materials Science & Processing

A. MARTUCCI[1,✉]
M. DE NUNTIS[1]
A. RIBAUDO[1]
M. GUGLIELMI[1]
S. PADOVANI[2]
F. ENRICHI[2]
G. MATTEI[2]
P. MAZZOLDI[2]
C. SADA[2]
E. TRAVE[2]
G. BATTAGLIN[3]
F. GONELLA[3]
E. BORSELLA[4]
M. FALCONIERI[5]
M. PATRINI[6]
J. FICK[7]

Silver-sensitized erbium-doped ion-exchanged sol–gel waveguides

[1] INSTM, Dipartimento di Ingegneria Meccanica S. Materiali, Università di Padova, Via Marzolo 9, 35131 Padova, Italy
[2] INFM, Dipartimento di Fisica, Università di Padova, Via Marzolo 8, 35131 Padova, Italy
[3] INFM, Dipartimento di Chimica Fisica, Università Ca' Foscari di Venezia, Dorsoduro 2137, 30123 Venezia, Italy
[4] ENEA-FIS, Via Enrico Fermi 45, 00044 Frascati, Italy
[5] ENEA, Unità Materiali e Nuove Tecnologie, C.R. Casaccia, Via Anguillarese 301, 00060 S. Maria di Galeria, Roma, Italy
[6] INFM, Dipartimento di Fisica 'A. Volta', Università di Pavia, Via Bassi 6, 7100 Pavia, Italy
[7] Laboratoire de Spectrométrie Physique, Université Joseph Fourier, 140 Avenue de la Physique, 38402 St. Martin d'Hères, France

Received: 20 April 2004/Accepted: 15 June 2004
Published online: 11 August 2004 •

ABSTRACT Ag- and Er-doped glass films have been synthesized with a combined sol–gel and ion-exchange route. The introduction of silver as erbium sensitizer in the film was obtained by ion exchanging Er-doped SiO_2–Al_2O_3–Na_2O sol–gel films. The films were subsequently annealed under controlled atmosphere to induce the migration and aggregation of the metal ions. Films showed different Er^{3+} photoluminescence behaviors depending on silver concentration and aggregation state. The interaction between erbium ions and Ag centers has been investigated and enhancement of the excitation cross section due to the silver sensitizing effect has been demonstrated. The developed synthesis also allowed the realization of erbium-doped channel waveguides by a selective Na–Ag ion-exchange process.

PACS 81.20.Fw; 78.55.-m; 42.82.Et

1 Introduction

Erbium-doped optical waveguides have received growing interest over the last decade due to their multiple applications, for example in integrated lasers or amplifiers for telecommunications [1]. One of the major limits to the application of rare earth doped glasses as optical amplifiers or solid-state lasers is related to the small absorption cross sections of rare-earth ions. To increase the Er^{3+} pumping efficiency many solutions have been investigated, such as co-doping with other rare earths like Yb [2] or by introducing broadband sensitizer species like organic complexes [3], Si nanocrystals [4–6] and metals [7, 8]. However, the mechanism that controls the enhancement of the Er^{3+} photoluminescence is still under debate. Regarding the silver sensitizing effects, it is not clear if the enhancement is due to the presence of silver clusters [8, 9] or to defects related to a pair of silver ions/atoms [7].

✉ Fax: +39-049/827-5505, E-mail: alex.martucci@unipd.it

Sol–gel is a very convenient technique for the fabrication of high-quality thin glass films and it is of great interest for industrial fabrication because of its low-cost availability and batch processing. Erbium-doped waveguides based on silica, silica–titania or phosphate glasses have been prepared with this technique. An overview of recent progress in this field is given in [10].

As the realization of an integrated optical amplifier requires confined waveguides, the glass composition of the thin-film material and the substrate plays a key role to produce the vertical confinement of light. Channel waveguides have been fabricated in sol–gel materials by laser densification [11], strip loaded and buried geometry [12, 13], UV–Vis densification [14] or ion exchange in bulk glasses [15]. Among these techniques, ion exchange represents probably the most simple and easy way to obtain the lateral confinement.

In this paper we report the synthesis and characterization of Ag and Er co-doped glass films. The introduction of silver as erbium sensitizer in the film was obtained by ion-exchanging Er-doped SiO_2–Al_2O_3–Na_2O sol–gel films. The films were subsequently annealed under controlled atmosphere to induce the migration and aggregation of the metal ions. Moreover, erbium-doped channel waveguides were also prepared by a selective ion-exchange process.

2 Experimental

Films of nominal molar composition $90\,SiO_2$ – $10\,Al_2O_3$ with different Na_2O content (3, 6 and 9 mol %) and doped with 0.5 mol % of Er have been synthesized by a sol–gel process. Tetraethyl orthosilicate $Si(OC_2H_5)_4$ (TEOS) and aluminum tri-sec-butoxide $[C_2H_5CH(CH_3)O]_3Al$ (ABO) have been used as precursors for silica and alumina, respectively. TEOS was dissolved in ethanol (EtOH) and hydrolyzed with H_2O and HCl (TEOS : EtOH : H_2O : HCl = 1 : 2.2 : 2 : 0.01, Sol.Si). ABO was mixed with ethanol and acetylacetone (acacH) under reflux at 70 °C (ABO : acacH : EtOH = 1 : 0.5 : 60, Sol.Al). Sodium acetate dissolved in methanol

(0.022 mg/l, Sol.Na) and erbium nitrate dissolved in ethanol (0.029 mg/l, Sol.Er) have been used as sodium and erbium precursors, respectively. The deposition solutions have been obtained by mixing Sol.Si, Sol.Al and Sol.Er at room temperature for 14 h, before adding Sol.Na.

Multi-layer films have been deposited on silica or silicon substrates by dipping. Each layer was annealed in air at 800 °C for 10 min. A final heat treatment in air at 1000 °C for 1 h was performed after the deposition of the last single layer. The typical thickness of each single layer after heat treatment was about 0.1 μm. By this process it is possible to realize crack-free films with up to 20 layers and a total thickness of about 2 μm.

The sol–gel samples containing 3, 6 and 9 mol % Na_2O are referred to as Er3, Er6 and Er9, respectively. In order to introduce silver in the Er-doped glass films, Na^+–Ag^+ ion exchange was performed on the Er3, Er6 and Er9 samples by immersing the films deposited on silica glass slides in a molten salt bath (1 mol % of $AgNO_3$ in $NaNO_3$) at 320 °C for 6 min. After the ion exchange, the samples containing 3, 6 and 9 mol % Na_2O are referred to as Er3Ag, Er6Ag and Er9Ag, respectively. Moreover, the Er9 films were also exchanged at 320 °C for 6 min in a molten salt bath with a higher concentration of silver (12 mol % of $AgNO_3$ in $NaNO_3$). In the following, they are referred to as Er9Ag(12). In order to promote silver aggregation, the ion-exchanged films have been heated at 500 °C in N_2 for 3 or 5 h.

Fourier-transform infrared (FTIR) measurements were performed on films deposited on silicon (Perkin Elmer 2000) in the range 400–4000 cm^{-1}.

Linear absorption spectra in the UV–Vis region (250–900 nm) were recorded at room temperature using a V570 Jasco spectrophotometer.

Compositional analyses were performed by means of an IMS 4f mass spectrometer (Cameca, Padova, Italy) using a 10-kV Cs^+ primary beam and by negative secondary ion detection (the sample potential was fixed at -4.5 kV) with a final impact energy of 14.5 keV. The SIMS (Secondary Ion Mass Spectroscopy) spectra were obtained in ultra high vacuum conditions at different primary beam intensities (50 nA and 75 nA) rastering over a nominally $125 \times 125\ \mu m^2$ area. The beam-blanking mode was used to improve the depth resolution, interrupting the sputtering process during magnet-stabilization periods. The dependence of the erosion speed on the matrix composition was taken into account by measuring the erosion speed at various depths in each sample. The erosion speed was then evaluated by measuring the depth of the erosion crater at the end of each analysis by means of a Tencor Alpha Step profilometer with a maximum uncertainty of a few nanometers. The measurements were performed in high mass resolution configuration to avoid mass-interference artefacts. The charge build-up while profiling the insulating samples was compensated by an electron gun without any need to cover the surface with a metal film.

Elemental concentration was obtained by Rutherford backscattering spectrometry (RBS) at INFN-Legnaro National Laboratories by using a 2.2-MeV $4He^+$ beam (backscattering angle = 160 degrees). SIMS raw data were converted to concentration profiles by normalization to the RBS doses. The resultant spectra were then compared to those given by the simulation program of the corresponding RBS spectrum, where SIMS raw data were used as input (the procedural details are reported elsewhere [16]). The agreement was found to be better than 4%, compatible with the error of RBS measurements.

Photoluminescence (PL) spectra were obtained by using a multi-line argon laser as excitation light source. The 488-nm wavelength (direct excitation for erbium) and the 476.5-nm wavelength (non-resonant excitation for erbium) were selected by specific filters. The power on the sample was set at 10 mW over a circular spot whose diameter was 1 mm. Periodic excitation and de-excitation of the sample were achieved by chopping the laser light with a mechanical chopper, with repetition frequency set at 10 Hz. The luminescence signal was analyzed by a single-grating monochromator equipped with a near-infrared photomultiplier tube cooled by nitrogen at a working temperature of −80 °C. To prevent the laser beam from reaching the detector, a 600-nm long-wavelength-pass filter was used at the monochromator entrance. The PL spectra were acquired with a lock-in amplifier using the chopper frequency as a reference, while for the time-resolved PL spectra the signal was sent to a transient digitizer and stored by a computer.

Photoluminescence excitation (PLE) spectra of the Er^{3+} 1.54-μm fluorescence emissions were measured at room temperature using a frequency-doubled Ti:sapphire laser that can be continuously tuned from 360 to 430 nm. The laser repetition rate was 10 Hz and the pulse width was 15 ns. The Er^{3+} emission was collected by a Cassegrain optics matched to a 18-cm effective focal length monochromator equipped with a 2-μm blazed grating. An AR/AR-coated silicon filter was inserted in the optical path to ensure rejection of visible light. The signal was detected by an InGaAs photodiode followed by a low-noise preamplifier. The time evolution of the emission was displayed and stored by a digital averaging oscilloscope.

The ellipsometric functions $\tan\psi$ and $\cos\Delta$ (with $\tilde{\varrho} = \tan\psi \exp(i\Delta)$, where $\tilde{\varrho}$ is the complex ratio of the parallel to the perpendicular polarization reflection coefficients) were measured between 250 and 900 nm by an automatic ellipsometer (Sopra ES4G). The system uses a 75-W xenon lamp, a rotating polarizer, an auto-tracking analyzer, a double monochromator and a single-photon-counting photomultiplier detector system. $\tan\psi$ and $\cos\Delta$ were measured with a typical standard deviation of less than 0.005, with a mesh of 2.5 nm and a spectral resolution of 0.25 nm, at two angles of incidence ($\phi = 75°$ and 70°) close to the Brewster angle for optimum sensitivity.

For the channel-waveguide fabrication, a 300-nm-thick aluminum film was evaporated on the Er3 films. By standard photolithography and wet-etching techniques straight waveguides of different widths were reproduced on this aluminum mask. The ion-exchange process was realized following the procedure of Er3Ag samples. After the ion-exchange process the mask was removed and the sample was cleaved to obtain good-quality end faces for waveguide characterization. The light was coupled by a monomode optical fiber and the near-field image was taken with an infrared camera by a microscope objective. For the loss measurements, the camera was replaced by a calibrated optical power meter. Pigtailed

laser diodes emitting at 1.02 μm were used for the characterization of the waveguiding properties.

3 Results

Compositional analysis performed on the sol–gel films shows that the distribution of all elements is almost constant through the film thickness, with a typical profile reported in Fig. 1. SIMS profiles were converted to concentration profiles by using the RBS doses. In Table 1 we report the average element concentrations. We observe that the interface between the film and the substrate remains quite sharp, the small in-diffusion of the species into the substrate being less than 100 nm. The film thickness varies in the range 1000–1600 nm depending on the preparation parameters. In particular, no segregation peak can be observed at the film–substrate interface.

From Table 1 it can be seen that erbium concentration is about 1×10^{20} at/cm^3 for all the analyzed samples, while the values of sodium concentration in Er3, Er6 and Er9 films (not reported in the table) are 3.9×10^{20}, 1.4×10^{21} and 3.1×10^{21} at/cm^3, respectively.

After the ion-exchange process, SIMS measurements show that the silver ions diffuse into the film, replacing a fraction of Na ions that out-diffuse into the molten salt. Depending on the starting bath composition, the Ag concentration changes. In the case of the 1 mol % $AgNO_3$ molten salts, in fact, the Ag concentration ranges from 8.9×10^{19} to 8.2×10^{20} at/cm^3, corresponding to a substitution of about 20% of the total sodium amount. Instead, by using the 12 mol % $AgNO_3$ molten salts, the Ag concentration reaches 2.5×10^{21} at/cm^3, corresponding to a substitution of about 80% of the total sodium amount.

In the FTIR spectra of the films heated at 1000 °C, reported in Fig. 2, no OH vibration bands (960, 1630 and 3000–3500 cm^{-1} [17]) have been observed for all the three compositions. The same behavior has also been observed after the introduction of silver in the sol–gel films. Absorption bands typical of silicate glasses have been observed around 800 and 1080 cm^{-1} with a shoulder at 1200 cm^{-1} [17].

The UV–Vis spectra showed no surface plasmon resonance band for all the investigated samples.

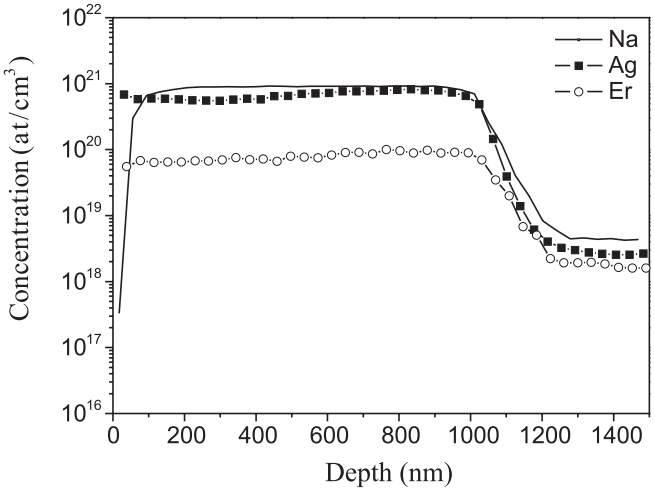

FIGURE 1 SIMS experimental profiles for the sample Er9Ag

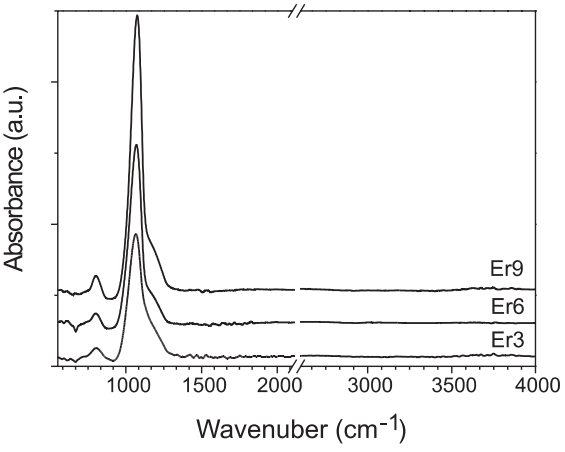

FIGURE 2 FTIR spectra of films heated at 1000 °C before ion exchange

The PL emission intensities, by excitation at both 488 and 476.5 nm, are reported in Table 2 for all the analyzed samples. These intensities were calculated as the integral of the emission spectrum and the signal was normalized to the thickness of the films. Moreover, it was normalized to the Er concentration after having been verified for all of the samples to be in a linear regime at the excitation power (10 mW) used. In

Sample	n (at 600 nm)	Ag concentration (at/cm^3)	Er concentration (at/cm^3)	Al/Na
Er3	1.467	0	9.2E+19	2.5
Er3Ag	1.476	8.9E+19	9.8E+19	
Er3Ag + N_2 (500 °C, 3 h)	n.m.	7.7E+19	9.1E+19	
Er3Ag + N_2 (500 °C, 5 h)	n.m.	7.7E+19	1.1E+20	
Er6	1.481	0	1.2E+20	1.6
Er6Ag	1.490	2.6E+20	9.5E+19	
Er6Ag + N_2 (500 °C, 3 h)	n.m.	1.8E+20	9.8E+19	
Er6Ag + N_2 (500 °C, 5 h)	n.m.	2.1E+20	9.6E+19	
Er9	1.494	0	1.0E+20	1.1
Er9Ag	1.499	8.2E+20	9.6E+19	
Er9Ag + N_2 (500 °C, 3 h)	n.m.	4.6E+20	8.1E+19	
Er9Ag + N_2 (500 °C, 5 h)	n.m.	3.7E+20	6.7E+19	
Er9Ag(12)	1.536	2.5E+21	1.0E+20	
Er9Ag(12) + N_2 (500 °C, 5 h)	n.m.	2.1E+21	8.0E+19	

TABLE 1 Refractive index n and Er and Ag concentrations for the analyzed samples. In the *last column* the ratio between Al and Na for the films before ion exchange is also reported

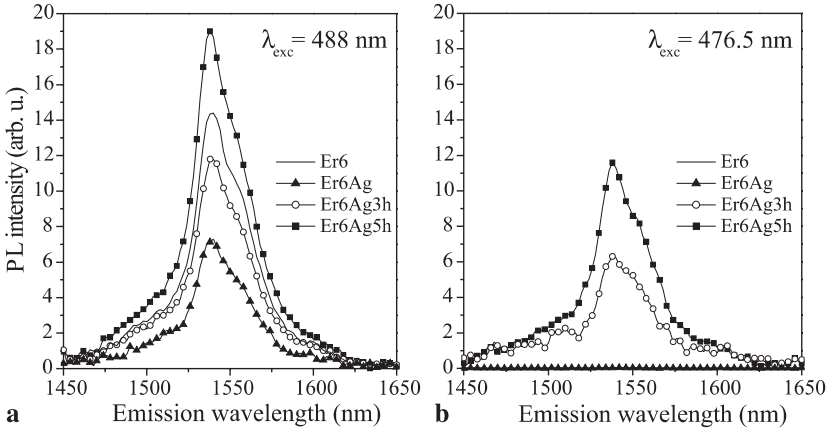

FIGURE 3 PL spectra for Er6, Er6Ag and Er6Ag heated at 500 °C in nitrogen for 3 h (Er6Ag3h) and 5 h (Er6Ag5h) measured by excitation at 488 nm (**a**) and 476.5 nm (**b**)

Sample	PL intensity ($\lambda_{exc} = 488$ nm)	PL intensity ($\lambda_{exc} = 476.5$ nm)	Lifetime (ms)
Er3	30	–	7.9
Er3Ag	24	–	7.4
Er3Ag + N_2 (500 °C, 3 h)	26	4	7.6
Er3Ag + N_2 (500 °C, 5 h)	36	13	7.7
Er6	19	–	10.6
Er6Ag	10	–	5.2
Er6Ag + N_2 (500 °C, 3 h)	16	8	6.2
Er6Ag + N_2 (500 °C, 5 h)	25	15	6.5
Er9	11	–	11.0
Er9Ag	6	–	7.7
Er9Ag + N_2 (500 °C, 3 h)	33	32	8.0
Er9Ag + N_2 (500 °C, 5 h)	35	37	8.2
Er9Ag(12)	11	5	6.1
Er9Ag(12) + N_2 (500 °C, 5 h)	56	55	7.6

TABLE 2 Photoluminescence intensity and lifetime for the analyzed samples

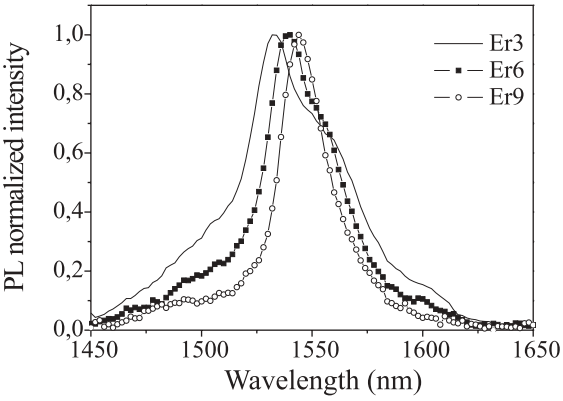

FIGURE 4 PL ($\lambda_{ex} = 488$ nm) normalized spectra for the samples Er3, Er6 and Er9

Table 2 the lifetime values are also reported, evaluated by fitting the decay curves with a single-exponential function. The values for the PL intensity and for the lifetime are affected by uncertainties of about 15% and 5%, respectively. As an example, the PL spectra for the series 6 samples are reported in Fig. 3, obtained with resonant at 488 nm (a) and non-resonant at 476.5 nm (b) excitation.

As far as non-exchanged films (Er3, Er6, and Er9), it is worth noting that:

- PL emission at 1.54 μm is detected only for resonant excitation (488 nm);
- by increasing the Na_2O concentration in the film (from 3 mol % to 9 mol %) the PL intensity decreases by a factor of three;
- lifetime values increase with the Na_2O concentration, following the opposite trend with respect to the intensity of the PL signal. From the single-exponential fitting of the decay curves, it was found that the lifetimes are 11.0 ms and 10.6 ms (typical values for erbium in silica glasses) for the samples Er9 and Er6, respectively, and 7.9 ms for the Er3 sample.

The normalized PL spectra, by excitation at 488 nm, for the samples Er3, Er6 and Er9 are reported in Fig. 4. The spectrum shape and emission-peak position vary with different concentrations of Na_2O in the film. In particular, the Er9 sample exhibits a narrower band (26 nm) with a unique peak at 1.544 μm. Instead, the sample with the lowest amount of Na_2O (sample Er3) exhibits a broader emission spectrum (52 nm) with the main peak shifted towards lower wavelength (1.532 μm) and a broad shoulder centered at about 1.553 μm. The emission spectrum for the Er6 sample has an intermediate feature with respect to the Er9 and Er3 spectra.

After the introduction of silver via the ion-exchange process, Ag is known to locate in the matrix mainly bonding with oxygen atoms [18–20], i.e. Ag–O pairs. As far as exchanged films (Er3Ag, Er6Ag, Er9Ag and Er9Ag(12)), it is worth noting that:

- Er3Ag, Er6Ag and Er9Ag films showed PL emission at 1.54 μm only for resonant excitation, while Er9Ag(12) films also showed non-resonant emission;
- for all the series, the introduction of silver in the doped layer induces a decrease of the resonant PL signal;
- the 1.54-μm emission lifetime decreases after the Na–Ag exchange process. In particular, the Er lifetime decreases from 7.9–11 ms for the non-exchanged samples (Er3, Er6 and Er9) to 5.2–7.4 ms for the exchanged samples (Er3Ag, Er6Ag, Er9Ag and Er9Ag(12)).

To further investigate the possible interaction between erbium ions and Ag centers, annealing treatments were performed. These post-exchange treatments are known, in fact, to promote Ag migration and aggregation [18–20]. From the data

reported in Table 2, the main observations that can be drawn are the following:

- after thermal treatments the PL signal rises, both for resonant and non-resonant excitation. The same behavior is observed for the decay lifetimes, which increase to 6.2–8.2 ms. Anyway, the lifetime of Ag-doped samples is always shorter than the non-exchanged one, even after 5-h annealing;
- thermal annealing at 500 °C in N_2 for 5 h of Er3Ag and Er6Ag films induces a slight increase of resonant PL intensity with respect to the non-exchanged films (Er3 and Er6), while Er9Ag annealed samples showed a resonant PL intensity three times larger than Er9 films;
- for the Er9Ag(12) sample the 5-h annealing induces an even higher increase of the resonant PL signal, which reaches an intensity value five times larger than the Er9 sample;
- Er9Ag annealed samples exhibit the same PL intensity for excitation at 476.5 nm and 488 nm;
- all the samples annealed for either 3 or 5 h exhibit non-resonant emission at 1.54 μm.

In Fig. 5 the PLE spectrum of the Er9Ag sample annealed for 5 h at 500 °C in nitrogen (Er9Ag5h) is reported and compared to the one obtained from the as-prepared one (Er9). If we focus attention on the sample without Ag, we can see that Er^{3+} ions can be excited only through direct absorption lines at 365, 378 and 406 nm, respectively. On the other hand, for the Er9Ag5h sample the PLE spectrum exhibits a non-zero signal even for non-resonant excitation, in the whole range 360–430 nm.

The experimental ellipsometric spectra were used to determine the refractive index $n(\lambda)$ in the transparency region (250–900 nm) and the actual thickness of the films by modeling the samples in a three-phase scheme (air–film–Si substrate), and imposing on $n(\lambda)$ the well-known Sellmeier dispersion relation:

$$n^2 = A + B\frac{\lambda^2}{\lambda^2 - C^2}\,, \tag{1}$$

where A, B and C are variable fit parameters. The spectra of $\tan\psi$ and $\cos\Delta$ at two different incidence angles were fitted simultaneously using the software package by Woollam, Inc., based on the Levenberg–Marquardt algorithm. The resulting $n(\lambda)$ spectra of some significant samples are reported in Fig. 6. The refractive-index values at $\lambda = 600$ nm of the films before and after ion exchange are reported in Table 1. For non-exchanged films (Er3, Er6 and Er9) the refractive index increases as the sodium concentration increases, and for ion-exchanged films (Er3Ag, Er6Ag, Er9Ag and Er9Ag(12)) the refractive index increases as the silver concentration increases. An index change (Δn) of 0.009 was obtained in Er3Ag and Er6Ag samples with respect to the films before ion exchange, while a Δn of 0.005 was obtained in the Er9Ag film. A much higher index change ($\Delta n = 0.042$) was obtained using a molten salt bath with a concentration of silver 12 times higher (Er9Ag(12)).

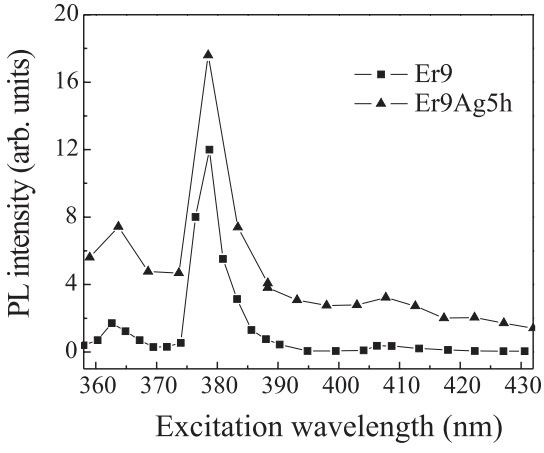

FIGURE 5 PLE spectra for the samples Er9 and Er9Ag heated for 5 h at 500 °C in nitrogen (Er9Ag5h)

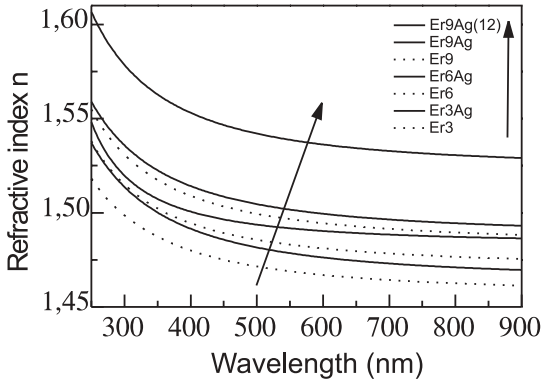

FIGURE 6 Refractive-index spectra of the films, derived from ellipsometry. Samples before and after ion exchange are indicated as *dotted* and *full lines*, respectively

A 1.5 μm in height by 9 μm in width channel waveguide was obtained after selective ion exchange. The channel waveguide was monomode at 1.02 μm with 3-dB/cm propagation losses and showed 1.54-μm fluorescence emissions of Er^{3+}.

4 Discussion

For the material preparation we chose a combination of a sol–gel technique and an ion-exchange process because this approach is very versatile for a fine tuning of the film compositions and optical properties. In this way it was possible to obtain Er-doped waveguides with different concentrations of Er and of Na_2O. Moreover, the Na–Ag ion-exchange process allows the study of the Ag-mediated energy-transfer mechanism avoiding the disadvantages of other preparation techniques such as, for example, the radiation damage induced by ion implantation.

A subsequent thermal treatment is used to modify the Ag local environment and to promote Ag aggregation. In fact, after Na–Ag ion exchange, Ag atoms are expected to be bound to non-bridging O atoms [20–22] since they substitute the Na atoms in the glass matrix. The developed technique also allows the realization of channel waveguides by selective ion exchange, which are the bases for the realization of optical integrated devices.

The resonant PL signal decrease, observed for all samples after Na–Ag ion exchange, may be related to the introduction of non-radiative centers due to the ion-exchange process

and to the modification of the local environment of erbium atoms. In fact, the silver atoms replace sodium ones, inducing a rearrangement of the glass structure. In agreement with this hypothesis, the 1.54-μm emission lifetimes of the samples decrease after the Ag^+–Na^+ exchange process, as reported in Table 2. In particular, the Er lifetime decreases from 7.9, 10.6 and 11 ms for Er3, Er6 and Er9, respectively, to 7.4, 5.2 and 7.7 ms for Er3Ag, Er6Ag and Er9Ag, respectively. As no variation in OH content has been observed in films before and after ion exchange, an OH quenching related process can be excluded. Increasing of both resonant PL intensity and decay lifetimes after heat treatments of the ion-exchanged samples were already observed by Fick et al. [21] in GeO_2–SiO_2 Na–Ag ion-exchanged sol–gel films. The different resonant PL intensity behaviors observed between the Er3Ag, Er6Ag and Er9Ag samples after 5-h annealing are probably related to the amount of silver in the film (see Table 1: Ag concentrations are 7.7×10^{19}, 2.1×10^{20} and 3.7×10^{20} at/cm^3, for Er3Ag, Er6Ag and Er9Ag 5-h annealed films, respectively). This hypothesis is also confirmed taking into account that the films ion exchanged in a more concentrated salt bath (see Table 1: Ag concentration is 2.1×10^{21} at/cm^3 for the Er9Ag(12) 5-h annealed film), which contain a higher content of silver, showed the highest increase of PL intensity.

The results obtained for non-resonant excitation can be explained with an energy-transfer process between the silver centers and erbium ions. As shown in a previous paper [20], the annealing process promotes thermal migration and aggregation of silver atoms in multimer structures that are responsible for the energy-transfer process [22]. In particular, for the Er9Ag and Er9Ag(12) samples, characterized by the highest PL enhancement, the annealed samples show the same PL intensity at 476.5 nm and 488 nm. This is a clear indication of a very efficient energy-transfer process, since in this case the direct pumping contribution is negligible with respect to the Ag-mediated path. On the other hand, for Er3Ag and Er6Ag annealed samples the ratio between the PL emission at 476.5 and 488 nm is less than 1, and this could be ascribed to a lower concentration of sensitizer elements.

An important parameter associated with the efficiency of the energy-transfer process is the excitation cross section of Er^{3+} ions in the Ag–Er co-doped glasses. To estimate its value we have studied the rise time of the PL intensity at 1.5-μm emission. The PL intensity is in general given by

$$I \propto \frac{N^*}{\tau_R}\,, \tag{2}$$

N^* being the concentration of excited Er ions and τ_R the radiative lifetime. When non-linear effects can be neglected, and the transfer time is much shorter than the decay lifetime of the system, the effective rate equation for Er excitation is

$$\frac{dN^*}{dt} = \sigma\varphi\left(N - N^*\right) - \frac{N^*}{\tau}\,, \tag{3}$$

where N is the Er content, φ the photon flux and σ the effective Er excitation cross section. τ is the decay time, taking into account both radiative and non-radiative processes. If the continuous-wave pumping laser is turned on at $t = 0$ the PL intensity, according to (2) and (3), increases with the following law:

$$I(t) = I_0\left\{1 - \exp\left[-\left(\sigma\varphi + \frac{1}{\tau}\right)t\right]\right\}\,, \tag{4}$$

with I_0 being the steady-state PL intensity. The rise time τ_{on} hence follows the relationship

$$\frac{1}{\tau_{on}} = \sigma\varphi + \frac{1}{\tau}\,. \tag{5}$$

Therefore, a measure of the rise time as a function of the φ photon flux will therefore give direct information on the excitation cross section. We have performed such measurements for the samples annealed for 5 h at 500 °C in N_2. These samples are chosen as they exhibit the maximum PL intensity value. Since we are interested in studying the energy-transfer process, these evaluations were done by using the 476.5-nm pumping wavelength. In this way we are sure that the emitting Er ions are only those excited by the Ag-mediated process. The obtained values for the Er ion excitation cross section, reported in Table 3, ranging from 1.2 to 1.6×10^{-17} cm^2, are almost constant for all the samples suggesting that the same physical process is occurring. Moreover, the obtained cross sections are much higher than that for direct absorption of Er^{3+} ions, which is of the order of 10^{-21} cm^2 in this glass [23], indicating the effective occurrence of energy transfer.

To better investigate the efficiency of the occurrence of an energy-transfer effect in the Ag and Er co-doped glass, PLE analysis was performed in the spectral range between 360 and 430 nm. The PLE results obtained for Er9 and Er9Ag 5-h samples (see Fig. 5) further confirm the efficiency of an Ag-mediated energy-transfer process. In fact, only after annealing (Er9Ag, 5-h sample) does the PLE spectrum exhibit a non-zero signal in the non-resonant region. This means that only the samples containing silver can be excited in the whole explored interval of wavelengths, while the samples not containing silver can be excited only through the direct absorption line (388 nm) of Er^{3+} ions. Silver pairs and clusters exhibit absorption features at 365 nm and 420 nm [24], respectively. The PLE spectrum of the Er9Ag 5-h film showed no band around 420 nm, indicating that the energy-transfer mechanism is not mediated by absorption via plasmonic resonance due to silver clusters, in accordance with the absorption spectra which showed no plasmon band. Instead, the possible presence of an absorption band due to Ag pairs cannot be detected as it overlaps the Er absorption transition $^4G_{11/2} \rightarrow {}^4I_{15/2}$. The hypothesis of an energy-transfer mechanism related to Ag multimers is also supported by spectroscopic investigation of

Sample	Cross section (cm^2)
Er3Ag + N_2 (500 °C, 5 h)	$(1.2 \pm 0.4) \times 10^{-17}$
Er6Ag + N_2 (500 °C, 5 h)	$(1.6 \pm 0.3) \times 10^{-17}$
Er9Ag + N_2 (500 °C, 5 h)	$(1.4 \pm 0.7) \times 10^{-17}$
Er9Ag(12) + N_2 (500 °C, 5 h)	$(1.4 \pm 0.2) \times 10^{-17}$

TABLE 3 Absorption cross-section values calculated at 476.5-nm excitation wavelength

luminescence of silver ion exchanged soda lime glass [25], which evidenced the emission of Ag pairs in the wavelength region corresponding to Er absorption.

As is well known, photoluminescence is a sensitive probe of the local environment of ions in a host matrix, as the Stark levels for each ion depend strongly on the local electric field generated by the surrounding atoms [26]. Modification of Stark levels is reflected in different spectral shape and peak position. In the case of Er-doped pure silica, the spectrum characteristic of the $^4I_{13/2} \rightarrow {}^4I_{15/2}$ transition in Er^{3+} is typically sharp (FWHM $\cong$ 20 nm) with a main peak at 1.535 μm and a side one at 1.551 μm [23]; the two peaks are the resolved Stark structure. For the examined Er–Ag co-doped glasses the emission spectra, reported in Fig. 4, are broader than the Er-doped pure silica, as a typical behavior of multicomponent glasses [23], and the spectrum shape and emission peak position vary with different concentrations of Na_2O in the film. This behavior may be explained with different Er environments for the Er3, Er6 and Er9 samples, which contain different amounts of Na_2O. On the other hand, the decrease of the PL intensity with the Na_2O content could also be due to different Er sites. In fact, sodium aluminosilicate (NAS) glasses showed physical changes as the Al/Na ratio passes through the equivalence point [27]. Several structural models have been proposed to explain these physical changes. For compositions with Al/Na < 1 aluminum acts as network formers and the aluminate tetrahedrons are charge compensated by the sodium. In glasses with Al/Na > 1, some of the aluminum changes from being tetrahedrally coordinated to being octahedrally coordinated. Alternatively, aluminum remains tetrahedrally coordinated over the entire Al/Na composition range and changes in the network topology, bond angles or formation of triclusters occur when the Al/Na ratio passes through the equivalence point. In any case, different structural units are present in glass with Al/Na > 1. More structural units produce a larger distribution of sites for rare-earth ions and hence a broadening of the photoluminescence peak emission. The Al/Na ratio is 2.5 for Er3 samples, while it is close to 1 for Er6 and Er9 samples, so different Er sites are expected to be present in Er3 films with respect to Er6 and Er9 films.

Sodium–silver exchange is one of the most commonly used ion-exchange techniques allowing a high index difference [28]. All the ion-exchanged films (Er3Ag, Er6Ag, Ar9Ag and Ar9Ag(12)) showed a variation of refractive index (Δn) which could be high enough for the realization of waveguides (see Table 1). In fact, channel waveguides were obtained by ion exchanging Er3 films. The measured high losses are probably due to the multi-deposition process carried out in open environment, which introduces inhomogeneity and other sources of scattering losses. Improvements in the film fabrication, in the masking and in the ion-exchange procedure should allow significant loss reduction.

In summary, erbium-doped waveguides sensitized with silver have been realized by a combination of a sol–gel technique and an ion-exchange process. The Ag-mediated energy-transfer mechanism has been studied and related to Ag pairs and not to silver clusters.

ACKNOWLEDGEMENTS This work has been supported by MURST – PRIN 2004.

REFERENCES

1 M. Federighi, I. Massarek, P.F. Trwoga: IEEE Photon. Technol. Lett. **5**, 227 (1993)
2 C. Strohhofer, A. Polman: J. Appl. Phys. **90**, 4314 (2001)
3 L.H. Slooff, A. van Blaaderen, A. Polman, G.A. Hebbink, S.I. Klink, F.C.J.M. van Veggel, D.N. Reinhoudt, J.W. Hofstraat: Appl. Phys. Lett. **91**, 3955 (2002)
4 P.G. Kik, M.L. Brongersma, A. Polman: Appl. Phys. Lett. **76**, 2325 (2000)
5 P.G. Kik, A. Polman: J. Appl. Phys. **88**, 1992 (2000)
6 G. Franzò, F. Iacona, V. Vinciguerra, F. Priolo: Mater. Sci. Eng. B **69–70**, 335 (2000)
7 C. Strohhofer, A. Polman: Appl. Phys. Lett. **81**, 1414 (2002)
8 T. Hayakava, S. Tamil Selvan, M. Nogami: J. Non-Cryst. Solids **259**, 16 (1999)
9 S.T. Selvan, T. Hayakawa, M. Nogami: J. Phys. Chem. B **103**, 7064 (1999)
10 G.C. Righini, M. Forastiere, M. Guglielmi, A. Martucci: Proc. SPIE **3280**, 57 (1998)
11 S. Pelli, G.C. Righini, A. Verciani, M. Guglielmi, A. Martucci, A. Scaglione: Proc. SPIE **2213**, 58 (1994)
12 E.M. Yeatman, K. Pita, M.M. Ahmad, A. Vannucci, A. Fiorello: J. Sol–Gel Sci. Technol. **13**, 517 (1998)
13 R.R.A. Syms, V.M. Schneider, W. Huang, M.M. Ahmad: Electron. Lett. **33**, 1216 (1997)
14 P. Coudry, J. Chisham, M.P. Andrews, S.I. Najafi: Opt. Eng. **36**, 1234 (1997)
15 C.Y. Li, Y.H. Kao, K. Hayashi, T. Takada, J.D. Mackenzie, K.I. Kang, S.G. Lee, N. Peygambarian, M. Yamane, G. Zhang, S.I. Najafi: Proc. SPIE **2288**, 151 (1994)
16 F. Gonella, F. Caccavale, A. Quaranta: Int. J. Optoelectron. **9**, 345 (1994)
17 P. Innocenzi: J. Non-Cryst. Solids **316**, 309 (2002)
18 G. Battaglin, E. Cattaruzza, F. Gonella, R. Polloni, F. D'Acapito, S. Colonna, G. Mattei, C. Maurizio, P. Mazzoldi, S. Padovani: Nucl. Instrum. Methods Phys. Res. B **200**, 185 (2003)
19 G.N. Greaves, S.J. Gurman, C.R. Catlows, A.V. Chadwick, S.N. Houde-Walter, C.M.B. Henderson, B.R. Dobson: Philos. Mag. A **64**, 1059 (1991)
20 F. D'Acapito, F. Gonella, E. Cattaruzza, S. Pascarelli, P. Mazzoldi, S. Mobilio: Nucl. Instrum. Methods Phys. Res. B **120**, 110 (1996)
21 J. Fick, A. Martucci, M. Guglielmi: J. Sol–Gel Sci. Technol. **19**, 573 (2000)
22 P. Mazzoldi, S. Padovani, F. Enrichi, G. Mattei, C. Sada, E. Trave, M. Guglielmi, A. Martucci, G. Battaglin, E. Cattaruzza, F. Gonella, C. Maurizio: Proc. SPIE **5451**: Integr. Opt. Photon. Integr. Circuits, in press
23 A. Polman: J. Appl. Phys. **82**, 1 (1997)
24 U. Kreibig, M. Vollmer: *Optical Properties of Metal Clusters* (Springer Ser. Mater. Sci. **25**) (Springer, Berlin 1995)
25 E. Borsella, F. Gonella, P. Mazzoldi, A. Quaranta, G. Battaglin, R. Polloni: Chem. Phys. Lett. **284**, 429 (1998)
26 P.M. Peters, S.N. Houde-Walter: J. Non-Cryst. Solids **239**, 162 (1998)
27 D.M. Zirl, S.H. Garofalini: J. Am. Ceram. Soc. **73**, 2848 (1990)
28 J.L. Jakel: Appl. Opt. **27**, 472 (1988)